Proceedings of the
Annual Stability Conference
Structural Stability Research Council
Louisville, Kentucky, April 1-4, 2025

Investigation on load transfer mechanisms in concrete-filled steel tubular (CFST) columns with beam shear connections

Weijie Ning[1], Partha P. Debnath[2], Tak-Ming Chan[3], Ahmed Y. Elghazouli[4]

Abstract
Concrete-filled steel tubular (CFST) compression members are widely used in the construction of buildings and bridges due to their superior ductility, higher load-carrying capacity, and ease of construction. For the CFST columns with welded shear connections, the load introduction into the CFST columns predominantly relies upon the interfacial bond behavior between the concrete core and the inner surface of the steel tube. However, this bond behavior is subject to numerous uncertainties and susceptible to alterations resulting from various parameters. Therefore, blind-bolted shear connections have been adopted in this study for effective load transfer, where the bearing of bolt shank on the steel tube and concrete core minimizes the dependency on bond strength for load transfer. A total of four full-scale specimens of CFST columns with shear connections were tested to investigate the load introduction mechanism. For this testing program, the parameters include, CFST compact and non-compact cross-section, and different connection types (welded connection and blind-bolted connection). Stub column tests for all the CFST cross-sections were also conducted to obtain cross-sectional resistance. From the experimental findings, it has been observed that, due to the bearing mechanism of the blind bolts in the bolted shear connection, the efficiency of load transfer was significantly enhanced compared to the specimen with welded connections. Full composite resistance for both compact and slender CFST columns with blind-bolted connections can be achieved, signifying effective load transfer and enhanced composite action. Finally, the provisions of the compressive strength for CFST composite columns from the international standards, AISC 360-22 and AS 2327, were evaluated based on the test results.

1. Introduction
Concrete-filled steel tubular (CFST) columns offer a range of advantages including increased load-bearing capacity, good ductility, and excellent fire resistance. The concrete core plays a crucial role in delaying the inward buckling of steel tubes, while the steel tube reinforces the strength and ductility of the concrete. Previous research has predominantly delved into investigating the structural behavior of isolated CFST columns (Dai & Lam, 2010; Ellobody & Young, 2006; Han et al., 2008), which assumes the attainment of composite action between the steel tube and concrete

[1] Ph.D. Candidate, The Hong Kong Polytechnic University, < weijie.ning@connect.polyu.hk >
[2] Post-doctoral Fellow, The University of Hong Kong, < parthapd@hku.hk >
[3] Professor, The University of Hong Kong, < tak-ming.chan@hku.hk >
[4] Chair Professor, The Hong Kong Polytechnic University, < ahmed.elghazouli@polyu.edu.hk >

core. However, in practical applications of CFST columns, external loads are not solely applied at the top of the column but also via beam connections, which can manifest as welded or bolted connections. Therefore, ensuring an effective transfer of applied loads from the steel tube to the concrete core, either through a natural bond or other transfer mechanisms, becomes imperative. In cases of CFST columns with welded connections, where the connections are attached solely to the steel wall, the load applied through connections gradually transfers from the steel tube to the column core via the bond mechanism at the steel-concrete interface. Existing research on the bond behavior of the CFST columns reveals the influence of various parameters such as tube dimensions, concrete strength, concrete shrinkage, and interface conditions (Morishita, 1979; O'Shea & Bridge, 2000; Qu et al., 2013; Roeder et al., 1999; Tomii, 1985; Virdi & PJ, 1980). However, no consistent conclusions have been reached regarding the effects of some crucial factors on bond behavior. Given the scarcity of research on bond behavior and the lack of consistent conclusions regarding the effects of various parameters on bond behavior, the reliability of bond strength for efficiently transferring load from welded beam connections to CFST columns raises significant concerns.

Several research studies have been undertaken to investigate the load transfer mechanisms in CFST columns featuring welded connections. Mollazadeh and Wang (2014) conducted experimental tests on the CFST columns with welded connections and observed that the CFST columns with limited length above the connection cannot achieve the full load transfer relying on the bond mechanism at the steel-concrete interface. Additionally, Xu et al. (2021) tested six CFST members with welded connections and found that the non-compact and slender CFST members failed to reach the full design strength. Based on the existing studies, it can be stated that CFST columns with welded connections may potentially fall short of attaining the designed compressive strength, particularly in non-compact and slender sections. Blind-bolts have emerged as a superior connection type for connecting the beam and CFST columns, allowing for tightening from the outside of hollow sections without accessing the other side of the bolt, and facilitating load transfer through the bearing mechanism of the bolt shank (Debnath & Chan, 2022). However, limited research exists on the load transfer mechanisms of CFST columns utilizing blind-bolted connections. Hence, this study aims to conduct an experimental investigation to explore the composite behavior and the load transfer efficiency of CFST columns with beam shear connections. Compact and non-compact sections were investigated in this test program, as well as considering welded and blind-bolted connections. Furthermore, the provisions for the compressive strength of CFST composite columns in different international standards were evaluated based on the test results.

2. Experimental investigations

A total of eight specimens were tested in the Structural Engineering Research Laboratory of The Hong Kong Polytechnic University. For load introduction tests, a set of four specimens, comprising two welded and two blind-bolted shear connections, were considered. Another set of four specimens was used for stub column tests, including two repeated specimens to obtain the cross-sectional capacity of the corresponding CFST columns.

2.1 Test specimens

The specimens for the load introduction tests considered two cross-section slenderness, which are regarded as compact and non-compact sections, classified based on the American standard

(ANSI/AISC, 2022). The limit values of the width-to-thickness ratio for box sections are presented in Table 1, where E and f_y is the elastic modulus and the yield strength of the steel tube, respectively. Therefore, the 200 × 200 square steel tubes with 5mm and 3mm thickness were prepared for the tests. The square steel sections were fabricated via welding two channel sections. As stated previously, two different shear connections were considered in the load introduction tests: welded and blind-bolted connections. For welded connections, fin plates were welded on two sides of the column to transfer the shear load. On the other hand, for the blind-bolted connections, twelve M20 Lindapter hollo-bolts (Lindapter, 2024) of grade 8.8 were used on each side for connecting the T-stub to the column, as depicted in Fig. 1. Both the welded and blind-bolted connections have been designed to possess higher capacity than the CFST columns, so that the total load introduced by the connections can be studied.

Table 2 summarizes the details of all the specimens, including the dimensions, the column length, the length above and below the connection, the connection length, the cross-section slenderness and the test types. As shown in Table 2, the specimens with a prefix of "SC" represent the columns for the stub columns, and the postfix of "R" means the repeated tests. The capital letters T, A, B, W and HB refer to the first letter of thickness, above, below, welded and hollo bolt, respectively. For example, the specimen T5-A200-B500-HB denotes a 200 × 200 square CFST columns with a 5 mm thickness of steel tube, which is fabricated with bolted connections using Hollo bolts. The length above and below the connection is 200 mm and 500 mm.

Table 1: Limiting width-to-thickness ratios for box sections

Width-to-thickness ratio	Compact/Non-compact sections (λ_p)	Non-compact/Slender sections (λ_r)	Maximum permitted
b/t	$2.26\sqrt{\frac{E}{f_y}}$	$3.00\sqrt{\frac{E}{f_y}}$	$5.00\sqrt{\frac{E}{f_y}}$

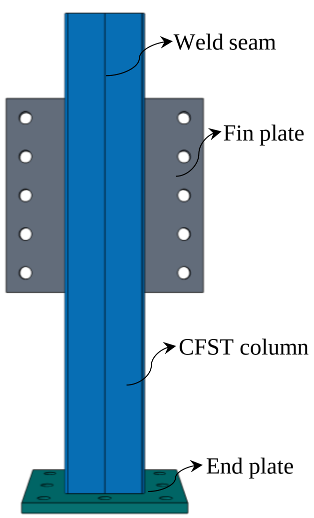

(a) Welded specimen

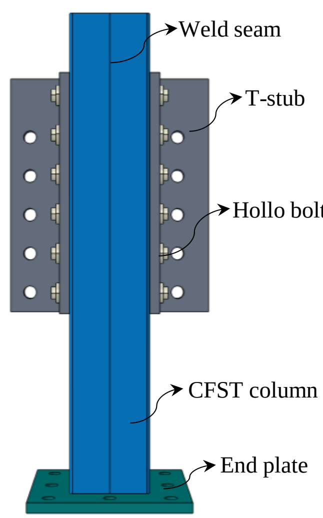

(b) Blind-bolted specimen

Figure 1: Details of the tested specimens

Table 2: The details of the test specimens

Specimen ID	Nominal dimensions (mm)					Slenderness classification	Test type
	$b \times b \times t$	L	L_A	L_B	L_C		
SC-T5	200 × 200 × 5	600	/	/	/	Compact	Stub column tests
SC-T5-R	200 × 200 × 5	600	/	/	/	Compact	
SC-T3	200 × 200 × 3	600	/	/	/	Non-compact	
SC-T3-R	200 × 200 × 3	600	/	/	/	Non-compact	
T5-A200-B500-W	200 × 200 × 5	1200	200	500	500	Compact	Load introduction tests
T5-A200-B500-HB	200 × 200 × 5	1200	200	500	500	Compact	
T3-A200-B500-W	200 × 200 × 3	1200	200	500	500	Non-compact	
T3-A200-B500-HB	200 × 200 × 3	1200	200	500	500	Non-compact	

Note: b is the width of the cross-section; t is the thickness of the cross-section; L is the column length; L_A is the length above the connection; L_B is the length below the connections; L_C is the length of the connection region.

The height of the fin plate in the welded specimen can be regarded as the connection length, on the other hand, for the bolted specimens, the connection length can be regarded as the distance between the center of the first row of bolts to that of the last row of the bolts and is kept at a constant value of 500 mm for all the specimens.

2.2 Material properties

There are three main parts composing the test specimen, which are steel tube, concrete core and hollo-bolts, thus, the material tests were conducted for these components respectively. To determine the material properties of the steel tube, three steel coupons were extracted from the parent steel plates for both 5mm and 3mm thicknesses. The dimensions of the coupons were design in accordance with ISO 6892-1:2019 (ISO, 2019), and the tensile coupon tests were conducted using the Instron Electromechanical Universal Testing Machine. Two white dots were made at the end of the extensometer distance on the tensile coupons in order to measure the strain via the advanced video extensometer. Moreover, two strain gauges were also attached to the coupon to obtain the more accurate elastic modulus. The tensile coupon tests were loaded by the displacement control method, and the loading process referred to the procedure proposed by Huang and Young (2014). Based on the tensile coupon test, the average value of the yield stress (f_y), ultimate stress (f_u) and the elastic modulus (E) for the steel tube with different thicknesses are summarized in Table 3.

Table 3: Material properties of the steel tube, bolt shank and sleeves

Components	f_y (N/mm^2)	f_u (N/mm^2)	E (N/mm^2)
Steel tube-5mm thickness	432.60	537.25	208120
Steel tube-3mm thickness	375.90	505.45	208630
Bolt shank	910.90	1013.86	201707
Bolt sleeve	333.93	493.71	/

For the hollo-bolt, three cylindrical coupons shaped from the bolt shank were tested to obtain the material properties. Furthermore, as the sleeve is an important part of hollo-bolt to take the shear load, the Rockwell hardness test was carried out to estimate the yield strength and ultimate strength of the sleeves. Before the tests, the sleeve was separated into four parts, and the tests were performed on the five points that located evenly. The material properties of bolt shank and sleeves were also listed in Table 3. Furthermore, the concrete cylinders with the standard size of 100 mm diameter and 200 mm length were casted, and wrapped with cling film during curing to replicate the conditions of the infilled concrete in CFST columns. Both compressive and split tests were carried out for three cylinders respectively to determine the material properties of the concrete. For the compressive tests, two strain gauges were affixed to the cylinder surface in order to obtain the elastic modulus of the concrete. According to the tests, the compressive strength, elastic modulus, and tensile strength of the concrete is 40.1 N/mm^2, 28899 N/mm^2 and 2.9 N/mm^2, respectively.

2.3 Test setup and instrumentations

The stub column tests and load introduction tests were conducted using the 25000 kN compression testing machine and the 10000 kN servo control multi-purpose testing system in the Hong Kong Polytechnic University, respectively. The test setup and instrumentations for both tests were described in the following sub-sections.

2.3.1 Compressive stub column tests

As there are two different cross-sections with compact and non-compact slenderness that were considered in the test program, four CFST stub column tests including two repeated tests were carried out. The nominal length of the stub column was designed to be three times of the width of the square sections, which is the appropriate length to avoid global buckling (Ziemian, 2010). As shown in Fig. 2 (a), a pair of specially designed stiffeners were installed at both ends of the column to prevent any possible premature buckling failure. The ends of the column were milled flat before testing to achieve the uniform loading.

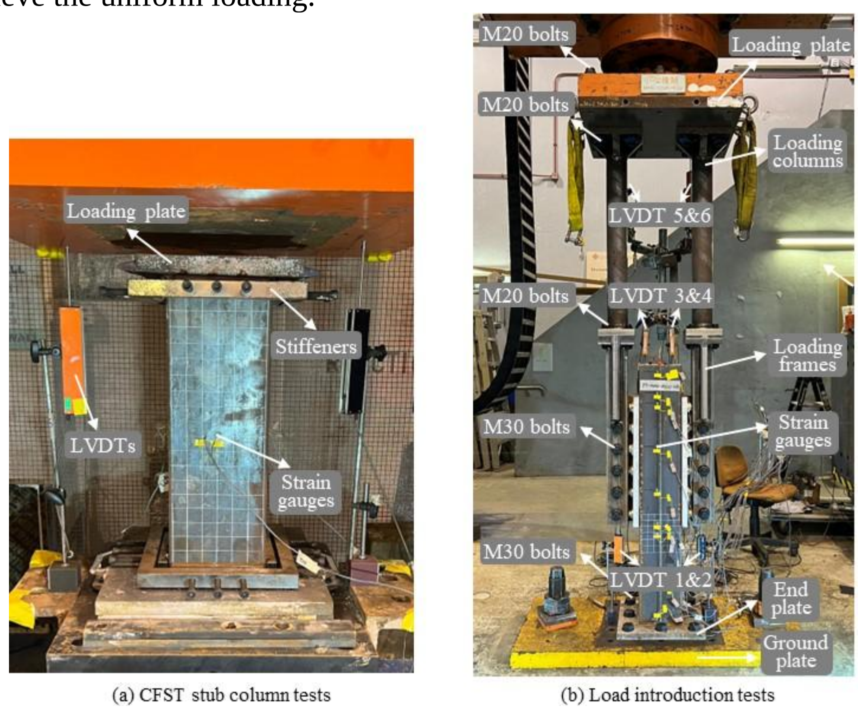

Figure 2: Test setup and instrumentations

To measure the end shortening of the stub column specimens, three 50 mm range Linear Variable Displacement Transducers (LVDTs) were placed on the left, right and rear sides respectively. Moreover, four strain gauges were attached to the mid-height of four faces to measure the longitudinal strain and monitor the initiation of local buckling. Additionally, the readings of the strain gauges were used to adjust the data obtained from LVDT measurements, eliminating the effects of initial gaps and deformation of the end plates, thus, providing more accurate end shortening of the specimen. The tests were performed by applying the load via displacement control method with a constant loading rate of 0.05% L mm/min (L is the length of the CFST column), which is similar to the rate used in tensile coupon tests prior to yielding. In order to ensure the LVDTs and strain gauges functioned properly and uniform loading, a preload of approximately 10% of the expected capacity was applied before the formal testing.

2.3.2 Load introduction tests

Totally, four load introduction tests were conducted considering the compact and non-compact sections, and different connection types. As shown in Fig. 2 (b), the specimens were installed on a rigid ground plate via the end plate welded on the bottom of the specimen, which was subsequently fixed with the strong floor. The shear load was applied through the T-stubs (for blind-bolted connections) or fin plates (for welded connections) on both sides, connected to the loading frames via M30 bolts of grade 10.9. The loading frames were then bolted with the solid circular high strength shafts (loading columns shown in Fig. 2 (b)), which were attached to the top loading plate. Finally, the axial load was applied through the central axis of the top plate to both connections. As the loading components will be used repeatedly, the yield loads for all the components have been designed to be approximately two times the capacity of the CFST specimens. Moreover, the shear and bearing capacity of the M30 bolts for connecting the fin plates and T-stubs have also been checked.

To obtain the displacements of the connections and the concrete core, two LVDTs were used respectively, as shown in Fig.2 (b). In addition, LVDT 5 and 6 were installed on the top loading plate to observe any possible gaps between the bolts and bolt holes. The longitudinal strains along the steel tube were measured utilizing the strain gauges attached to the front and right sides of the tube in different regions, specifically the regions above and below the connection, as well as the connection region. Most of the strain gauges were positioned at intervals of 200 mm; however, to monitor strains in critical areas, such as the region just above and below the connection, additional strain gauges were installed at these locations. Furthermore, in order to measure the strain distribution in the infilled concrete, a steel bar was placed at the center of the steel tube before casting the concrete. Strain gauges were attached to the steel bar evenly, protected by waterproof tape. At the beginning of the test, a preload of 50 kN was applied to eliminate the slip caused by the bolts for connecting the loading components and check the instrumentations. During the test, a loading rate of 0.3 mm/min was used for all the specimens. The tests were terminated upon either a 20% reduction in the ultimate load or when the measurements from LVDT 1 or LVDT 2 reached 15 mm, depending on which condition occurred first.

3. Analysis of the test results

According to the CFST stub column tests, the average of the ultimate loads for the stub columns with 5 mm and 3 mm thicknesses is 3060 kN and 2128 kN, respectively, which implies the cross-sectional capacity when achieving the composite action of the CFST columns. For the load introduction tests, the failure modes for the four specimens are shown in Fig.3. For all the specimens, with different cross-sectional slenderness and connection types, the failure occurs at the region below the connection part due to the local buckling of the steel tubes and is presented in Fig. 3 (a) – (c). Moreover, for the specimen with welded connections, an obvious slip between the steel tube and concrete core can be observed, which can be referred from Fig.3 (d), where the top surface of the concrete has a higher level than that of the steel tube. It indicates that, for welded shear connection specimens, the steel-concrete interfacial bond is crucial for effective load transfer.

The relationship between the load and displacement for the load introduction specimens is depicted in Fig. 4. The displacement shown as the horizontal axis in Fig.4 is the average readings of the LVDT 1 and 2. In addition, the ultimate loads collected from the experimental stub column tests and load introduction tests are listed in Table 4. The stub column tests and load introduction tests are indicated as subscripts “SC” and “test”, respectively. As shown in Fig.4, the horizontal dotted line represents the cross-sectional resistance load obtained from the CFST stub column tests, denoted as $N_{u,\,SC}$. It can be observed that the ultimate capacity for the specimens with welded connections falls short of attaining the cross-sectional capacity, indicating an incomplete composite action between the steel tube and infilled concrete. As illustrated in Table 4, only 79 % of the expected resistance can be achieved for the compact specimen with welded connections, while the non-compact specimens with welded connections achieve a mere 52%. It is attributed to the inferior bond stress at the steel-concrete interface in non-compact sections compared to the compact sections. However, for the specimens with blind-bolted shear connections, the ultimate load exceeds the value of stub column tests. This indicates that, using the blind-bolts instead of the welded connections, the load from connections can be fully transferred into the CFST columns, which significantly improves the efficiency of introducing the load for the shear connections.

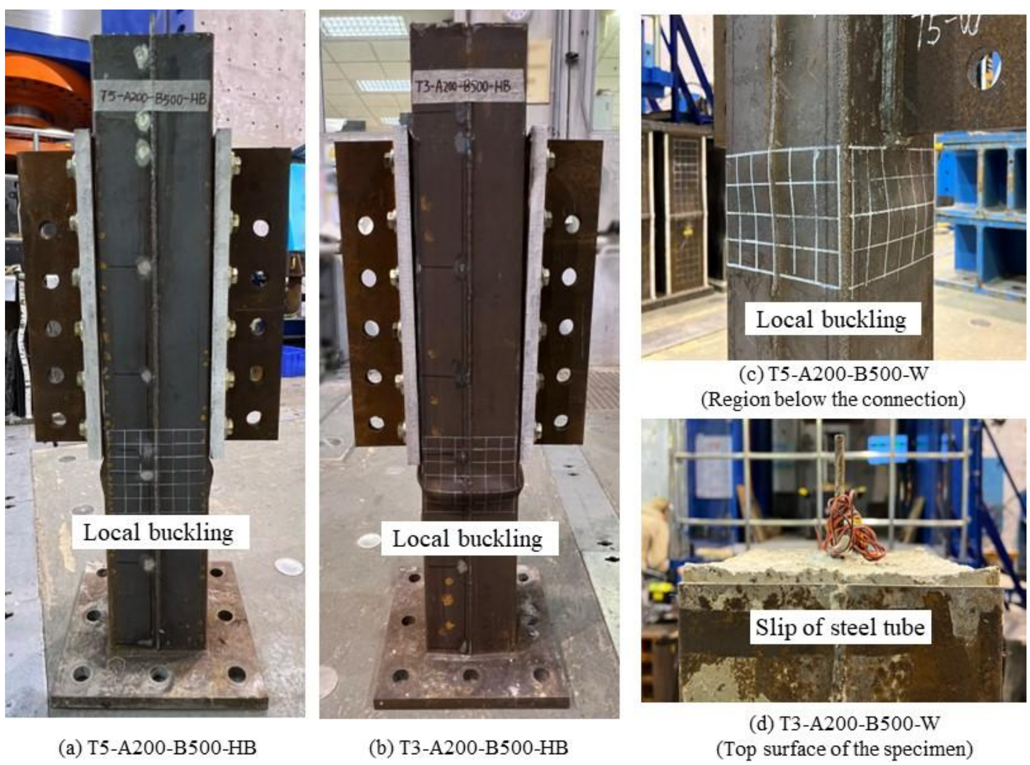

Figure 3: Failure modes for load introduction tests.

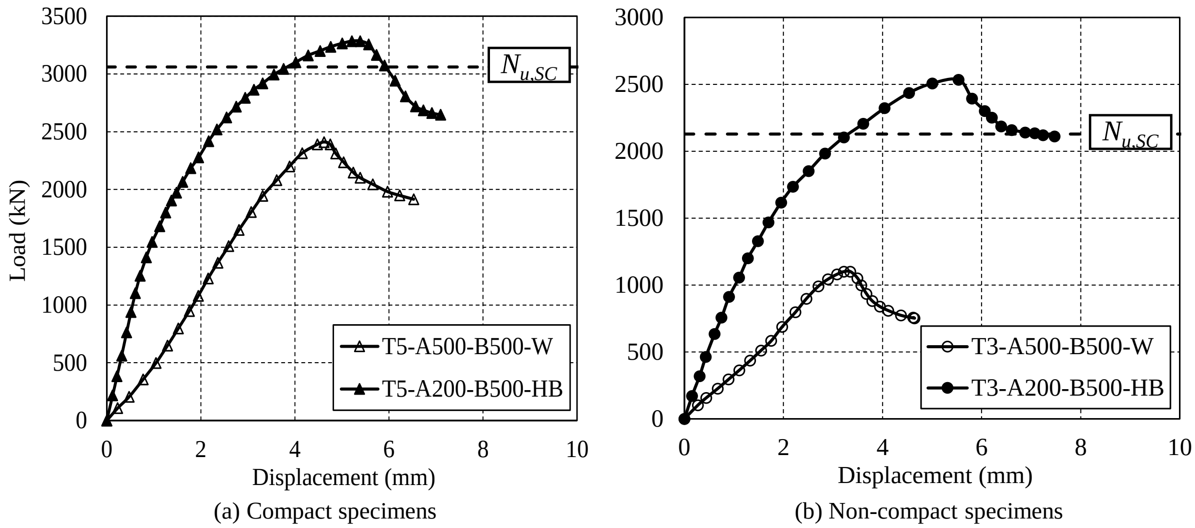

Figure 4: Load-displacement relationships of the load introduction tests.

Table 4: Comparison of results of experimental tests and design codes.

Specimen ID	$N_{u,test}$	$N_{u,SC}$	$N_{u,AISC}$	$N_{u,AS}$	$\frac{N_{u,test}}{N_{u,SC}}$	$\frac{N_{u,test}}{N_{u,AISC}}$	$\frac{N_{u,test}}{N_{u,AS}}$
T5-A200-B500-W	2411	3060	2881	3098	0.79	0.84	0.78
T5-A200-B500-HB	3285	3060	2881	3098	1.07	1.14	1.06
T3-A200-B500-W	1100	2128	2102	2285	0.52	0.52	0.48
T3-A200-B500-HB	2535	2128	2102	2285	1.19	1.21	1.11

Additionally, strain measurements were acquired for both steel tube and concrete core, which are summarized in Fig. 5 to Fig.8. The arrangement of the strain gauges is shown on the left side of each figure. Moreover, the relationship between the axial load and the micro strain for different sections is also depicted, with positive strain denoting under compressive stresses. Strain data from different regions are differentiated by color: blue, green, and red represent strain gauges above, within, and below the connection region, respectively. As shown in Fig. 5 and Fig.6, the larger strain value is observed for the region just below the connection for all the specimens, which indicates the presence of outward buckling in the steel tube at that specific location.

Notably, in Fig. 6, for the specimens with blind-bolted connections, the maximum strain below the connection is around 5000 με, whereas for the welded specimens depicted in Fig.5, the maximum strain can reach up to 6000 με. The difference implies a more effective transfer of load from the steel tube to the concrete core in the blind-bolted specimens, consequently restraining the buckling of the steel tube in comparison to the welded specimens. Furthermore, for all the specimens, the steel strain beneath the connection region can reach the steel yield strain, indicating the complete yielding of the steel tube. The strain data, depicted by blue curves, reveal negative values for strains above the connection, suggesting tensile stress in the steel tube resulting from shear resistance at the steel-concrete interface.

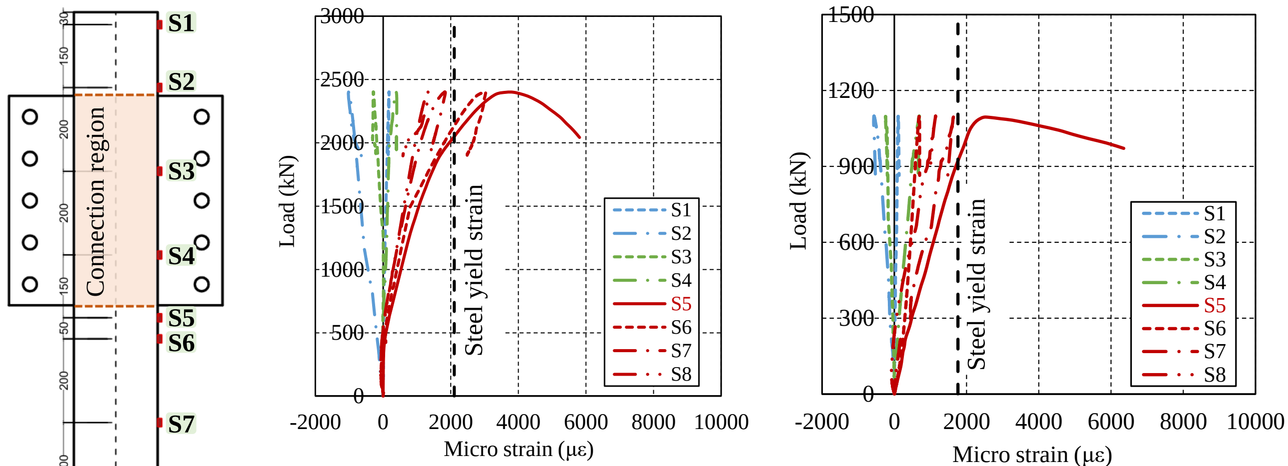

(a) T5-A200-B500-W
(Compact section)

(b) T3-A200-B500-W
(Non-compact section)

Figure 5: Steel strain for specimens with welded connection.

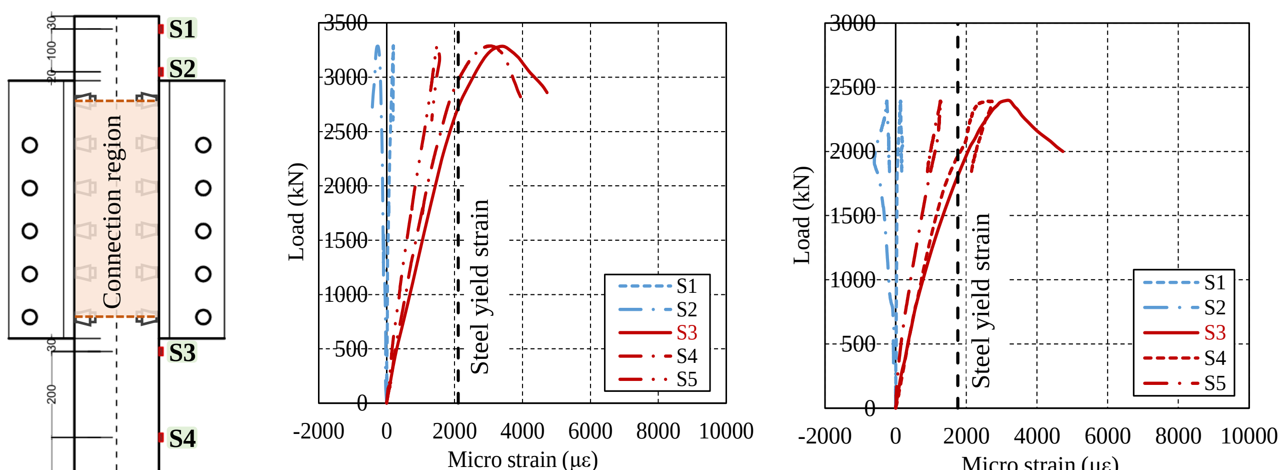

(a) T5-A200-B500-HB
(Compact section)

(b) T3-A200-B500-HB
(Non-compact section)

Figure 6: Steel strain for specimens with blind-bolted connection.

As depicted in Fig. 7, the maximum strain in the concrete core is localized at the region below the connection, which is 1105 με and 606 με for compact and non-compact sections respectively. Nevertheless, it has not achieved the concrete strain at peak stress (1389 με) for both different cross-sections. A noticeable disparity in the maximum concrete strain is evident between the compact and non-compact sections, with the former exhibiting enhanced bonding behavior, facilitating increased load transfer into the concrete core.

Fig. 8 illustrates the concrete strain in the specimens featuring blind-bolted connections. It is worth mentioning that, both the blind-bolted specimens have reached the concrete strain at peak stress, signifying the attainment of complete composite action between the steel tube and concrete core. Compared to the results for the welded specimens, it can be concluded that the blind-bolted connections can enhance the efficiency of load transfer between the steel tube and infilled concrete.

In the case of the compact section, it can be observed that the concrete strain has achieved the peak value even within the connection area, while for the non-compact section, the full strain is observable only beneath the connection region. The test results suggest that optimal composite action can be attained with blind-bolted connections in conjunction with compact sections.

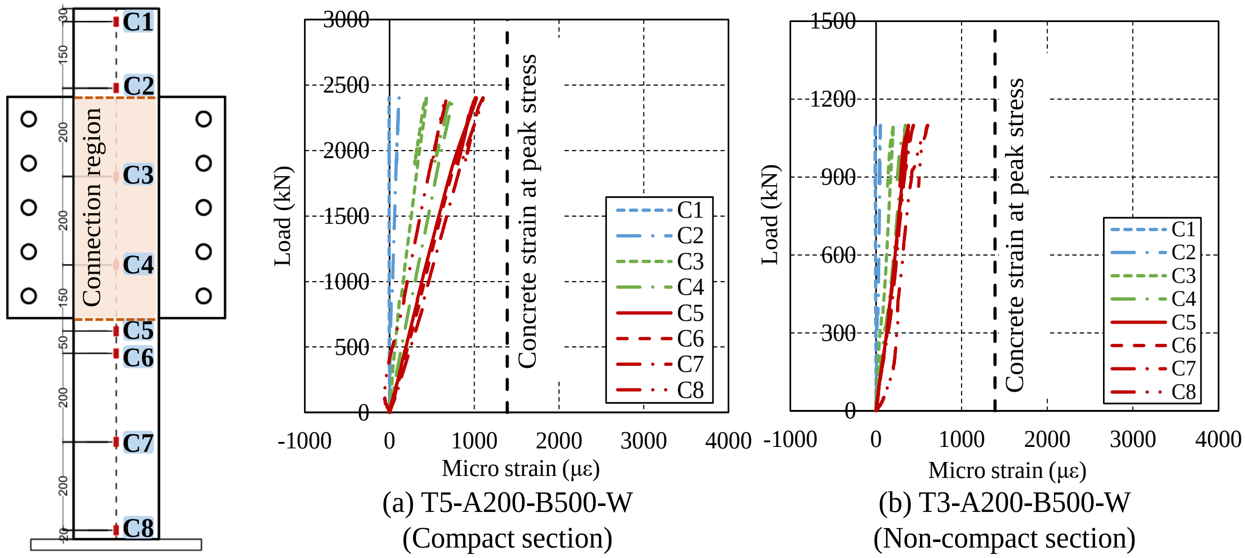

Figure 7: Concrete strain for specimens with welded connection.

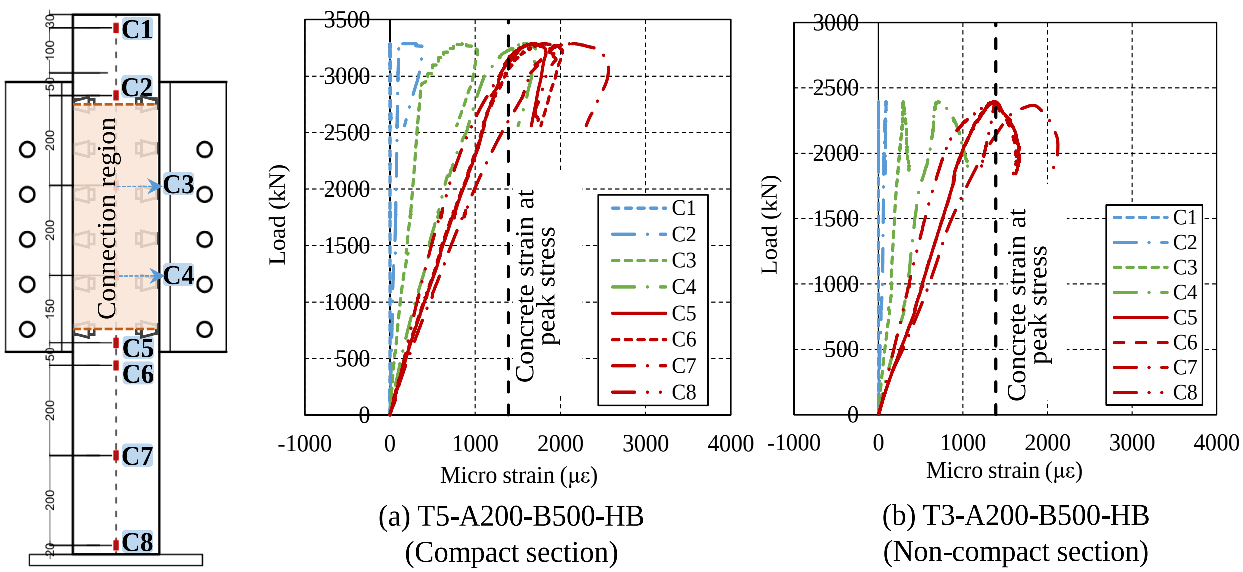

Figure 8: Concrete strain for specimens with blind-bolted connection.

4. Comparisons with the existing design guides

Various standards have been utilized to calculate the compressive strength of the CFST column. This section provides a summary of the equations derived from the American code AISC 360-22 (ANSI/AISC, 2022) and Australia code AS 2327 (AS/NZS, 2017), which are subsequently compared with the experimental test results. The compressive strengths proposed by the standards are denoted as “AISC” and “AS” for the subscript, respectively.

4.1 AISC 360-22

For the square compact composite sections, the compressive strength can be calculated by Eq.1:

$$N_{u,AISC} = N_p = f_y A_s + C_2 f_c A_c \tag{1}$$

where N_p is the plastic axial compressive strength, f_y is the steel yield stress, f_c is the concrete compressive strength, A_s and A_c is the area of the steel tube and concrete core, respectively, and C_2 is 0.85 for rectangular sections.

For non-compact sections, Eq.2 is used to determine the compressive strength:

$$N_{u,AISC} = N_p - \frac{N_p - N_y}{(\lambda_r - \lambda_p)^2}(\lambda - \lambda_p)^2 \tag{2}$$

where N_p can be calculated using Eq.1, λ_p and λ_r is the width-to-thickness ratio shown in Table 1, λ is the width-to-thickness ratio of the cross-section, and N_y is determined from Eq.3.

$$N_y = f_y A_s + 0.7 f_c A_c \tag{3}$$

4.2 AS 2327

In Australia code AS 2327, the provisions for calculating the compressive strength are the same for different cross-sections, which is determined as Eq.4:

$$N_{u,AS} = k_f f_y A_s + f_c A_c \tag{4}$$

where k_f is defined as the form factor to consider the local buckling effect, calculated by Eq.5:

$$k_f = \frac{A_e}{A_g} \tag{5}$$

where A_g is the gross area of the cross-section, and A_e is the effective area, which is determined by adding the effective area of individual elements calculated by the effective width (b_e). For square sections, the effective width can be obtained from Eq. 6.

$$b_e = b\frac{\lambda_{ey}}{\lambda_e} \leq b \tag{6}$$

where b is clear width of the steel plate, λ_{ey} is the width-to-thickness ratio to classify non-compact and slender sections in Table 1 as same as the American code, and λ_e is the slenderness defined as Eq. 7:

$$\lambda_e = \frac{b}{t}\sqrt{\left(\frac{f_y}{250}\right)} \tag{7}$$

where t is the thickness of the steel plate.

4.3 Summary and comparison of the results

According to the equations in the American and Australian codes as outlined previously, the compressive strength values of the CFST columns calculated from the respective standards have been listed in Table 4. It can be observed that the results from AS 2327 exhibit higher values for all the specimens in contrast to those derived from AISC 360-22. Furthermore, the Australian code demonstrates closer alignment with the ultimate loads obtained from the experimental stub column tests. Conversely, the strength of CFST columns with blind-bolted connections sees enhancement owing to the bearing mechanism of the blind-bolts. Consequently, as shown in Table 4, both standards underestimate the strength of the blind-bolted specimens, particularly evident in the case of the American code. Therefore, there is potential for optimization of the American and Australian standards for the CFST columns with different beam connections to refine the accuracy of determining column strength in subsequent investigations.

5. Conclusions

A laboratory experimental program has been conducted to explore load transfer mechanisms in concrete-filled steel tubular (CFST) columns featuring beam shear connections. The test specimens encompassed varying slenderness ratios (compact and non-compact sections) and connection types (welded and blind-bolted connections). The following important conclusions can be drawn:

(a) Compared with the cross-sectional resistance obtained from the experimental stub column tests, the CFST columns with welded connections fell short of attaining the full compressive strength, while their blind-bolted counterparts achieved the expected strength, indicating the complete composite action and enhanced load transfer efficiency facilitated by the bearing mechanism of blind bolts.

(b) Analysis of strain data from the steel tube and concrete for welded connections unveiled a higher concrete contribution in load transfer for compact composite sections as compared to non-compact composite sections. This indicates that, cross-sectional slenderness can influence the load introduction in CFST columns with welded shear connections.

(c) The research compared the test results with the compressive strength provisions for CFST composite columns outlined in AISC 360-22 and AS 2327 standards. Results indicated an overestimation of the compressive strength in CFST columns with welded connections by both standards, while strength in blind-bolted CFST columns was underestimated. Consequently, for improved accuracy in determining the compressive strength of CFST columns, further optimization of the provisions in both standards is warranted in subsequent investigations.

Acknowledgments

The authors would like to acknowledge the support of the technical team of Mr. Henry Cheung, Mr. Wa Hung Ng and Mr. Man Chuen Ng at the Structural Engineering Research Laboratory of The Hong Kong Polytechnic University; and graduate students Mr. Xiangyu Zhang of The Hong Kong Polytechnic University, and Mr. Cheng Zhang of The University of Hong Kong.

References

ANSI/AISC. (2022). ANSI/AISC 360-22: Specification for structural steel buildings.

AS/NZS. (2017). AS/NZS 2327: Composite Structures-Composite Steel-Concrete Construction in Buildings.

Dai, X., & Lam, D. (2010). Numerical modelling of the axial compressive behaviour of short concrete-filled elliptical steel columns. Journal of Constructional Steel Research, 66(7), 931-942.

Debnath, P. P., & Chan, T.-M. (2022). Experimental performance of single blind-bolted CFST column connection under predominant shear loading. Journal of Constructional Steel Research, 196, 107386.

Ellobody, E., & Young, B. (2006). Nonlinear analysis of concrete-filled steel SHS and RHS columns. Thin-walled structures, 44(8), 919-930.

Han, L.-H., Liu, W., & Yang, Y.-F. (2008). Behaviour of concrete-filled steel tubular stub columns subjected to axially local compression. Journal of Constructional Steel Research, 64(4), 377-387.

Huang, Y., & Young, B. (2014). The art of coupon tests. Journal of Constructional Steel Research, 96, 159-175.

ISO. (2019). ISO 6892-1:2019 Metallic materials - Tensile testing - Part 1: Method of test at room temperature.

Lindapter. (2024). https://www.lindapter.com/product/type-hb-hollo-bolt-hexagonal-head. Retrieved 12/03/2024 from

Mollazadeh, M. H., & Wang, Y. C. (2014). New insights into the mechanism of load introduction into concrete-filled steel tubular column through shear connection. Engineering Structures, 75, 139-151.

Morishita, Y. (1979). Experimental studies on bond strength in concrete filled circular steel tubular columns subjected to axial loads. Transactions of the Japan Concrete Institute, 1, 351-358.

O'Shea, M. D., & Bridge, R. Q. (2000). Design of Circular Thin-Walled Concrete Filled Steel Tubes. Journal of structural engineering (New York, N.Y.), 126(11), 1295-1303. https://doi.org/10.1061/(ASCE)0733-9445(2000)126:11(1295)

Qu, X., Chen, Z., Nethercot, D. A., Gardner, L., & Theofanous, M. (2013). Load-reversed push-out tests on rectangular CFST columns. Journal of Constructional Steel Research, 81, 35-43.

Roeder, C. W., Cameron, B., & Brown, C. B. (1999). Composite action in concrete filled tubes. Journal of structural engineering, 125(5), 477-484.

Tomii, M. (1985). Bond check for concrete-filled steel tubular columns. Effects of Damage and Redundancy on Structural Performance,

Virdi, K., & PJ, D. (1980). Bond strength in concrete filled steel tubes.

Xu, F., Song, S.-S., Lai, Z., & Chen, J. (2021). Mechanism of load introduction and transfer within steel-encased CFST members with shear connections. Engineering Structures, 242. https://doi.org/10.1016/j.engstruct.2021.112576

Ziemian, R. D. (2010). Guide to stability design criteria for metal structures. John Wiley & Sons.